Received: 11 January 2018 | Revised: 28 March 2018 | Accepted: 30 April 2018

DOI: 10.1002/JPER.18-0026

JOURNAL OF Periodontology

ORIGINAL ARTICLE

P53 mediates lipopolysaccharide-induced inflammation in human gingival fibroblasts

Jia Liu[1] | Jiajun Zeng[1] | Xiaoxuan Wang[1] | Ming Zheng[2] | Qingxian Luan[1]

[1]Department of Periodontology, Peking University School and Hospital of Stomatology, Beijing, P.R. China

[2]Department of Physiology and Pathophysiology, Peking University Health Science Center, Beijing, P.R. China

Correspondence
Qingxian Luan, Department of Periodontology, Peking University School and Hospital of Stomatology, No. 22 South Zhongguancun, Avenue, Haidian District, Beijing, 100081, P. R. China.
E-mail: kqluanqx@126.com

Ming Zheng, Department of Physiology and Pathophysiology, Peking University Health Science Center, No.38 Xueyuan Road, Haidian District, Beijing, 100191, P. R. China.
E-mail: zhengm@bjmu.edu.cn

Abstract

Background: The role of reactive oxygen species (ROS) in activation of the inflammatory response has been proven in previous study using human gingival fibroblasts (HGFs) to lipopolysaccharide (LPS) from *Porphyromonas gingivalis (Pg)* stimulation, but its exact mechanism has not been established. ROS can be generated through increased oxidative phosphorylation. P53 originally identified as a tumor suppressor, has been demonstrated to be associated with energy metabolism. We proposed that LPS-induced inflammatory cytokines release in HGFs is mediated by interaction between P53 and ROS levels.

Methods: HGFs were grown in medium with *Pg* LPS stimulation. Gene expression was performed by quantitative reverse transcription polymerase chain reaction (qRT-PCR) and Western blot analysis. HGFs were also processed by immunofluorescence to characterize the localization of P53. ROS was measured using a multimodal microplate reader and immunofluorescence microscopy. Cellular respiration levels were performed with a high-resolution respirometer. Cytokines secretion was confirmed by enzyme-linked immunosorbent assay.

Results: LPS-induced P53 activity and localization in mitochondria led to cellular redox imbalance and mitochondrial dysfunction, thus triggered the cellular inflammatory response with increased secretion of interleukin (IL)-1β, IL-6 and tumor necrosis factor (TNF)-α. Furthermore, the cellular redox imbalance and inflammation induced by LPS were reversed by inhibiting P53 activity. P53 expression followed by LPS-induced inflammation was also be restricted by suppressing ROS generation.

Conclusions: The present study shows that LPS-induced inflammation in HGFs is partially dependent on P53 modulating ROS and ROS stimulating P53, which suggests that P53 and ROS may form a feedback loop. The identification of this mechanism may provide potential new therapeutic strategies for periodontitis.

KEYWORDS

cell biology, cytokines, fibroblasts, oxidative stress, periodontitis, reactive oxygen species (ROS)

Periodontitis is an inflammatory disease characterized by alveolar bone destruction, which eventually contributes to tooth loss.[1] Evidence has shown that a majority of adults suffer from mild to moderate periodontitis.[2,3] Research on the pathogenesis of periodontitis and development of the new therapeutic approaches is therefore necessary. Periodontitis is initially induced by the colonization of different microorganisms in subgingival biofilm.[4] In this process, soft and hard tissue supporting the tooth is damaged. Human gingival fibroblasts (HGFs) are the major components of gingival connective tissue.[5] They recognize infection and are endowed with potent antimicrobial mechanisms. Meanwhile,

they also participate in the human immune response, leading to connective tissue destruction.[5]

Molecular mechanisms for the microorganism-mediated pathogenesis of periodontitis have been proposed. In the classical mechanism, lipopolysaccharide (LPS) from gram-negative bacteria contributes to the release of proinflammatory cytokines detected at lesion sites.[6] Studies demonstrated that bacterial stimuli induces periodontitis through reactive oxygen species (ROS) production, especially mitochondrial (mt)ROS generation.[7,8] In this mechanism, mtROS act as cellular signaling molecules, activating proinflammatory pathways.[9–11] Furthermore, inhibiting ROS release is accomplished by preventing LPS-induced mitogen-activated protein kinase (MAPK) and nuclear factor (NF)-κB activation, which are both essential steps in mediating periodontitis.[11] Therefore, mtROS play a supportive role in the initiation and development of periodontitis. They also serve as bridge signals that enable mitochondrial functions to be associated with periodontitis.[12,13]

A previous study demonstrated that ROS production is promoted by increased oxidative phosphorylation (OXPHOS).[14] P53 is involved in this mechanism through mediation of glycolysis and OXPHOS.[15–17] In this way, ROS production is altered and contributes to distinct cellular responses. A vital metabolic function of P53 is to augment mitochondrial respiration.[18] During this process, P53 is believed to directly or indirectly influence the expression of several enzymes participating in cellular respiration.[19,20] One example is mitochondrial pyruvate dehydrogenase (PDH) kinase 2 (PDK2), which is a negative regulator of PDH[19] and can lead to PDH activity inhibition. P53 inhibits PDK2 expression and promotes conversion of pyruvate to acetyl-coenzyme A (CoA),[19] which enhances cellular respiration. However, the mechanism connecting P53 to ROS and inflammation in HGFs has not been described.

Previous evidence has suggested that P53 is a vital mediator of inflammatory processes in disease.[21–24] The responses of P53 are context-specific and partially dependent on its expression and localization. In this study, we proposed that LPS from *Porphyromonas gingivalis* triggered inflammatory cytokine generation in HGFs by promoting redox imbalance with P53 involvement. We aimed to demonstrate a novel P53-mediated mechanism of LPS-induced inflammation, this may provide additional insights into P53 and periodontitis.

1 | MATERIALS AND METHODS

1.1 | Human gingival fibroblast culture

Primary HGFs were obtained from 4 patients (2 male and 2 female average age 35 years) without gingival or periodontal disease during crown-lengthening surgery. Sample collection was performed after receiving approval from the Review Board and Ethics Committee of Peking University Health Science Center (PKUSSIRB-2013017). Written, informed consent for tissue use was provided for the involved patients. HGFs were maintained in Dulbecco's modified Eagle's medium (Hyclone Laboratories, Logan, UT) (DMEM) supplemented with 10% fetal bovine serum (Gibco, Thermo Fisher Scientific, USA) (FBS) and 1% penicillin/streptomycin. They were cultured in the presence of 5% CO2 at 37°C. HGFs were used from passage 3 to 8.

1.2 | LPS/pifithrin-α/N-acetylcysteine treatment of HGFs

Cells plated in 6-well or confocal dishes were incubated to approximately 80% confluence. Cells were then stimulated with or without a P53 inhibitor (Pifithrin-α, Sigma-Aldrich, St. Louis, MO) (pifithrin-α) at a concentration of 20 μM for 2 h. Meanwhile another group of cells were culturing in the presence or absence of 1mM N-acetylcysteine (NAC) (Sigma-Aldrich, St. Louis, MO) for 1h. After washing with phosphate-buffered saline (PBS), 1 μg/mL *P. gingivalis* LPS (ATCCs 33277, InvivoGen, France) was added into the medium specified above. Untreated cells were used as a control. After that, cells and culture supernatants were collected for subsequent experiments.

1.3 | Transfection with P53 siRNA

Human P53 siRNA and scrambled control siRNA (Santa Cruz Biotechnology) were used for transfection. HGFs were transfected with 10 nM P53 siRNA or scrambled control siRNA using Lipofectamine RNAiMAX (Lipofectamine RNAiMAX, Thermo Fisher Scientific) according to the manufacturer's instructions. Cells were used 48 hours post-transfection and then treated with 1 μg/mL of LPS. The transfection efficiency was determined through Western blots by comparisons with control siRNA, and the efficiency exceeded 50%.

1.4 | Quantitative reverse transcription polymerase chain reaction (qRT-PCR)

Total RNA was extracted using TRIzol (TRIzol, Life Technologies, Thermo Fisher Scientific), and cDNA was synthesized by reverse transcription using qPCR RT Master Mix (ReverTra Ace, Toyobo, Osaka, Japan). Real-time PCR was performed using gene-specific primers and the qPCR Mix (Toyobo THUNDERBIRD SYBR, Toyobo, Osaka, Japan) on a PikoReal 96 real-time PCR system. Primers used were as follows: P53 (TCCTCCCCAACATCTTATCC and GCACAAACACGAACCTCAAA), PDK2 (ATGGCAGTCCTCCTCTCTGA and CACCCACCCTCTTCCTAACA), and GAPDH (GGAGCGAGATCCCTCCAAAAT and

GGCTGTTGTCATACTTCTCATGG). All samples were prepared in triplicate, and the relative mRNA expression in each sample was normalized to that of glyceraldehyde-3-phosphate dehydrogenase (GAPDH).

1.5 | Western blots

Equal amounts of protein from each sample (15–30 μg) was denatured and loaded onto 12% sodium dodecyl sulfate-polyacrylamide gels for electrophoresis (SDS-PAGE). The proteins were then transferred to nitrocellulose membranes (BD Biosciences, Franklin Lakes, NJ) and incubated blocking buffer containing 10% skim milk. Next, western blotting was carried out with primary antibodies against human P53 (Cell Signaling Technology, Danvers, MA) and p-P53 (Cell Signaling Technology) (at 1:1000 dilution), PDK2 (Abcam, Cambridge, UK) (at 1:1000 dilution), and horseradish peroxidase (HRP)-coupled anti-rabbit secondary antibody (Cell Signaling Technology) (at 1:2000 dilution) for detection. Finally, the bands were stained with an enhanced chemiluminescence kit. Rabbit anti-GAPDH was used as a loading control (Cell Signaling Technology).

1.6 | ROS production

The level of cytoplasmic ROS production in HGFs was assessed with 2′,7′-dichlorodihydrofluorescein diacetate (Sigma-Aldrich, St. Louis, MO) (H2DCF-DA). Cells were pre-incubated with H2DCF-DA (10 μM) for 30 minute at 37°C in 5% CO2. H2DCF-DA diffuses into cells and then is oxidized into the fluorescent compound 2′,7′-dichlorofluorescin (DCF). The fluorescence intensity under various conditions was measured as optical density (OD) at 488 nm with a multimodal microplate reader (EnSpire, PerkinElmer, Waltham, MA). Fluorescence was also measured by immunofluorescence microscopy (TCS-SP82; Leica, Wetzlar, Germany) with excitation and emission wavelengths of 488 nm and 535 nm, respectively

1.7 | Mitochondrial ROS production

HGFs were pre-incubated with 5 μM MitoSOX Red (Invitrogen, Carlsbad, CA) for 30 minute at 37°C in 5% CO2. MitoSOX Red is a superoxide-sensitive and mitochondria-specific targeted fluorescent probe that detects superoxide in the mitochondria of living cells. Once in mitochondria, MitoSOX Red is oxidized into a red fluorescent compound by superoxide. The fluorescence intensity of individual cells was measured by a multimodal microplate reader (EnSpire, PerkinElmer) at 510 nm and by immunofluorescence microscopy (Leica) with excitation and emission wavelengths of 510 nm and 580 nm, respectively.

1.8 | Mitochondrial membrane potential assessment

Mitochondrial membrane potential was measured with tetramethylrhodamine methyl ester (Invitrogen) (TMRM). Cells were plated onto confocal dishes in growth medium. A loading solution with 200 nM TMRM dye was added for 15 minutes at 37°C in 5% CO2. Afterwards, the dishes were gently washed twice with PBS. The fluorescence intensity of the samples was analyzed by immunofluorescence microscopy (TCS-SP82; Leica) with excitation and emission wavelengths of 549 m, and 573 nm, respectively.

1.9 | Cytokine measurements

Human IL-1β, IL-6, and tumor necrosis factor (TNF)-α enzyme-linked immunosorbent assay (ELISA) kits (R&D Systems, Minneapolis, MN) were used to measure the amounts of IL-1β, IL-6, and TNF-α secreted in culture supernatants according to the manufacturer's instructions.

1.10 | Respiration assays

Cellular respiration assays were performed with a high-resolution respirometer (Oxygraph-2K; Oroboros Instruments Corp, Innsbruck, Austria) to monitor basal respiration and maximal respiration activity according to the manufacturer's instructions. HGFs were pre-incubated with pifithrin-α for 2 hours. Afterwards, cells were cultured in growth medium with or without LPS treatment. On termination, about 1.5×10^6 HGFs were injected into each chamber of the respirometer before the addition of oligomycin, carbonyl cyanide 4-(trifluoromethoxy) phenylhydrazone (FCCP), rotenone, and antimycin A at the listed concentrations (Figure 4) Cellular basal respiration and maximal respiration activity were then analyzed based on these parameters.

1.11 | Immunofluorescence for colocalization analysis

HGFs were plated on confocal dishes. After LPS stimulation with or without pifithrin-α pre-incubation, cells were treated with 200 nM MitoTracker Red (Invitrogen) for 30 minutes at 37°C in 5% CO2, and then washed 3 times with PBS. For P53 protein (Toyobo Thunderbird SYBR, Toyobo, Osaka, Japan}staining, cells were fixed in 4% paraformaldehyde (PFA) for 15 minutes at 37°C and permeabilized for 10 minutes at 37°C in 0.2% Triton X-100 in PBS. Cells were then treated with blocking buffer (5% BSA in PBS) for 30 minutes at 37°C. Next, the samples were incubated with primary antibody to P53 (1:1600) diluted in 1% BSA for 2 hours at 37°C. Cells were washed 3 times with PBS, and then incubated with goat anti-rabbit Andy Fluor 488 secondary antibody (GeneCopoeia, Rockville, MD) for 1.5 hours at 37°C

before mounting with 4′6-diamidino-2-phenylindole (DAPI). The stained samples were evaluated under a 63 × 1.35 NA oil-immersion lens using a spinning-disk confocal microscope (Leica). P53 localization and mitochondrial colocalization percentages were measured using the "colocalization rate" in the LAS X software (Leica).

1.12 | Statistical analysis

All data were analyzed using GraphPad Prism (GraphPad, Inc, La Jolla, CA). Results are presented as means ± SE. Statistical significance between 2 samples was determined by Student's t-test, whereas ANOVA followed by Student Knewman-Keuls post hoc test were used to determine the difference among multiple comparisons. Differences were considered significant at $P < 0.05$.

2 | RESULTS

2.1 | LPS stimulation activated P53 and suppressed PDK2 in HGFs

Our previous study demonstrated that HGFs responded to LPS stimulation, which induced pro-inflammatory cytokine secretion by activation of mtROS.[8] We hypothesized that P53 regulates energy metabolism, resulting in ROS generation during this process. To validate this hypothesis, we assessed the expression of P53, p-P53, and PDK2, which is a negative regulator of PDH in cellular respiration. RT-PCR and western blots revealed expression of P53 and PDK2 at the RNA and protein levels respectively in LPS-treated HGFs. We observed that LPS stimulation increased P53 and p-P53 expression but decreased PDK2 expression (Figure 1).

We evaluated the function of P53 with a specific antagonist of P53 expression, pifithrin-α, and with transfection by P53 siRNA cultured with or without LPS. Consistently with the aforementioned results, pifithrin-α application or P53 siRNA combined with LPS stimulation both decreased cellular P53 at the RNA and protein levels, however PDK2 was observed slightly enhanced compared with that detected in LPS stimulated HGFs (Figure 1). Therefore, our results suggested that LPS stimulation of HGFs induced P53 activation and PDK2 suppression; additionally, P53 activation inhibits PDK2 expression.

2.2 | LPS treatment induced P53 accumulation in mitochondria and mitochondrial membrane potential destruction

Previous studies have demonstrated that mitochondrial membrane potential is destroyed by LPS stimulation and that P53 localization in cells on various stimuli plays an important role in mediating cell fates.[25] We therefore determined whether LPS treatment contributed to P53 localization and variation in mitochondrial membrane potential. To this end, HGFs were pre-cultured in the presence or absence of pifithrin-α, a specific inhibitor of P53, for 2 h, followed by stimulation with LPS. We found that P53 markedly translocated into the mitochondria on LPS stimulation (Figure 2). Treatment with the P53 inhibitor reversed P53 colocalization with mitochondria even after LPS stimulation (Figure 2).

LPS stimulation significantly reduced mitochondrial membrane potential in HGFs, and inhibition of P53 by Pifithrin-α pretreatment restored the potential to some extent (Figure 2). These results suggested that substantial loss of mitochondrial membrane potential by LPS treatment was possibly mediated by interactions between P53 and mitochondria.

2.3 | Activation of P53 regulated cellular respiration thus increased ROS levels in HGFs; ROS generation simultaneously enhanced P53 levels

To investigate the effects of P53 on ROS generation, we measured the cytoplasmic and mitochondrial ROS levels and cellular respiration in HGFs with LPS stimulation together with or without P53 inhibition by pifithrin-α/P53 siRNA and in control cells. To assess the influence of ROS on P53, we determined the levels of P53 expression on exposure to antioxidants such as NAC. Consistent with our previous results, levels of both forms of ROS were significantly higher in LPS-treated groups than those in control groups (Figure 3). Further, P53 inhibition combined with LPS stimulation reduced ROS levels compared to levels measured in LPS-stimulation alone (Figure 3). After suppressing ROS generation associated with LPS stimulation, the expression of P53 protein decreased significantly compared with that from the LPS-treated group. (Figure 3).

We next evaluated the differences in cellular respiration ability among LPS-treated, P53-inhibited with or without LPS stimulation, and untreated HGFs. Cellular respiration was amplified by LPS stimulation compared with that in the control group. As expected, we also found that cellular respiration was apparently reduced by LPS stimulation combined with P53 inhibition compared with that in cells treated with LPS alone (Figure 4).

2.4 | Proinflammatory cytokine secretion was significantly upregulated by LPS stimulation and downregulated by pifithrin-α (Pif-α) or NAC addition together with LPS stimulation in HGFs

Because we demonstrated the involvement of P53 in ROS signaling and mitochondrial function. Besides, ROS levels can influence P53 expression. We next investigated if P53 and

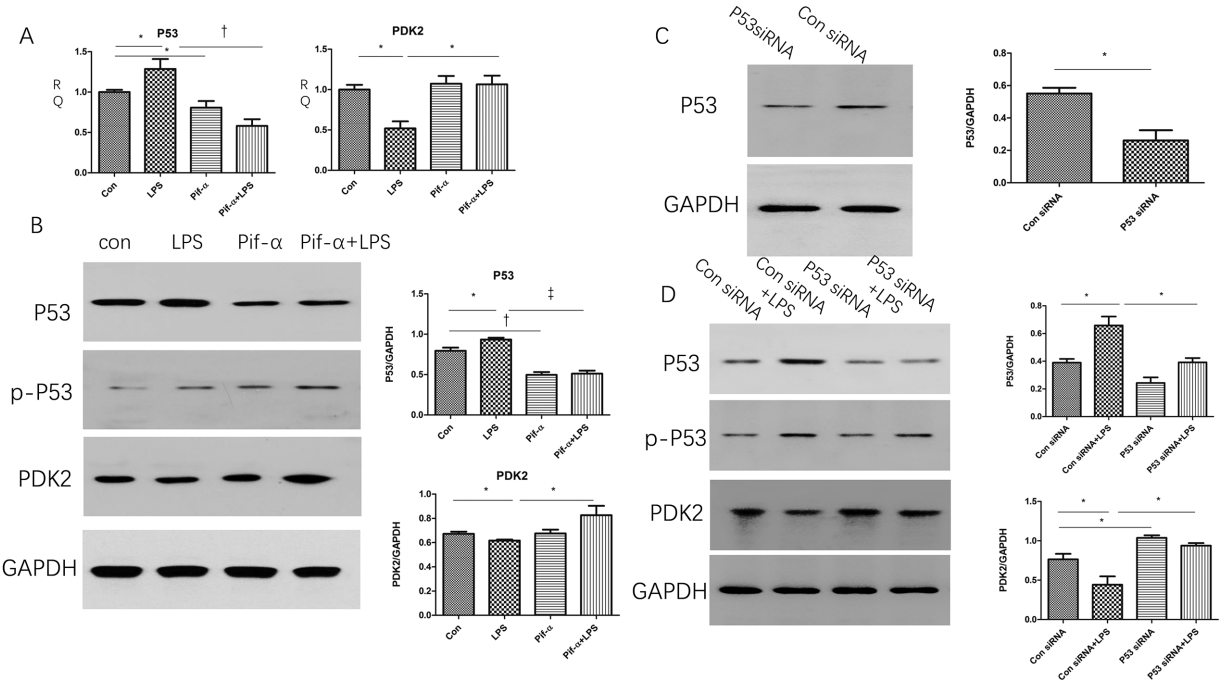

FIGURE 1 LPS stimulation activated P53 and suppressed PDK2 in HGFs. Human gingival fibroblasts were pretreated with 20 μM Pifithrin-α (Pif-α) or (C) transfected with P53 or control siRNA as described in Methods and then treated with 1μg/ml lipopolysaccharides (LPS) from *Porphyromonas gingivalis* (*P. gingivalis*) for 12 hours. (A) P53 and PDK2 mRNA expression was determined by quantitative real-time polymerase chain reaction (PCR) and normalized to GAPDH expression levels. (B and D) expression of P53, p-P53 and PDK2 protein was analyzed using Western blotting. Results were further quantified by densitometric analysis, normalized by the level of GAPDH. Experiments were repeated 3 times with human gingival fibroblasts. The presented data represented the mean±SE of results from 3 independent experiments performed on HGFs (Statistical significance between 2 means was determined by Student's *t*-test, whereas multiple comparisons were analyzed by ANOVA). RQ: relative quantity, $^{*}P < 0.05$, $^{\dagger}P < 0.01$, $^{\ddagger}P < 0.001$

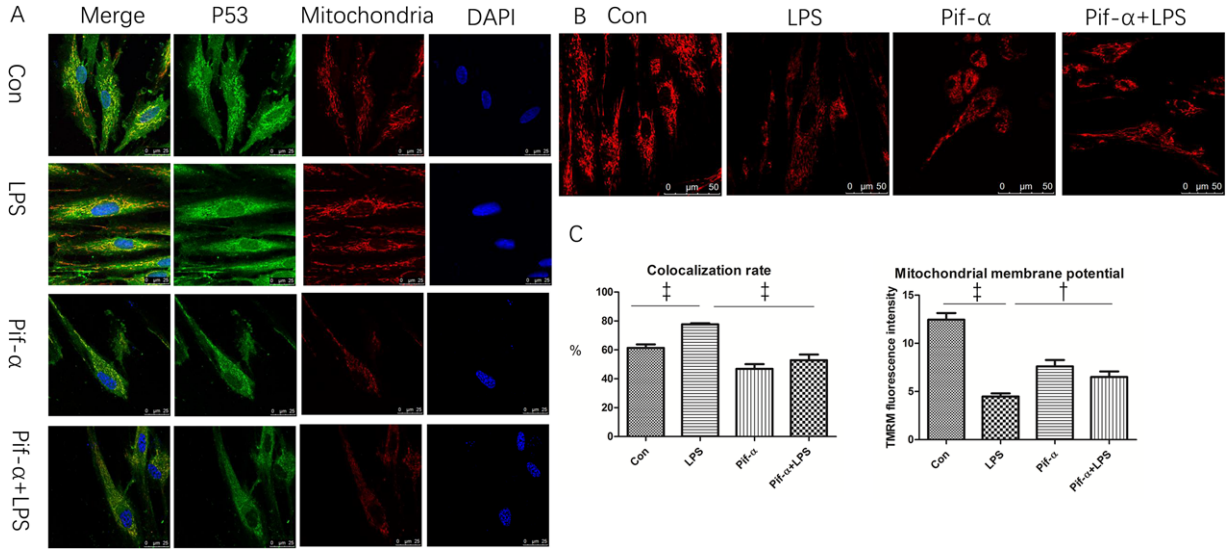

FIGURE 2 LPS treatment induced P53 accumulation in mitochondria and mitochondrial membrane potential destruction. (A) Distribution of P53 (green), mitochondria (red), and nucleus (blue) in HGFs. The merged insets in HGFs stimulated with LPS evidenced strong colocalization (yellow) of P53 with mitochondria in contrast with control group. Inhibition of P53 reduced this colocalization. The signal was detected using fluorescence microscopy. Scale bar, 25 μm. (B) LPS-treated HGFs reduced mitochondrial membrane potential compared with control group, whereas inhibition P53 with Pif-α reversed the weak signal. Scale bar, 50 μm. (C) counted at least 25 cells in each group. Compared the colocalization rate and mitochondrial membrane potential with data expressed as mean ± SE of 3 independent experiments (multiple comparisons were analyzed by ANOVA). $^{\dagger}P < 0.01$, $^{\ddagger}P < 0.001$

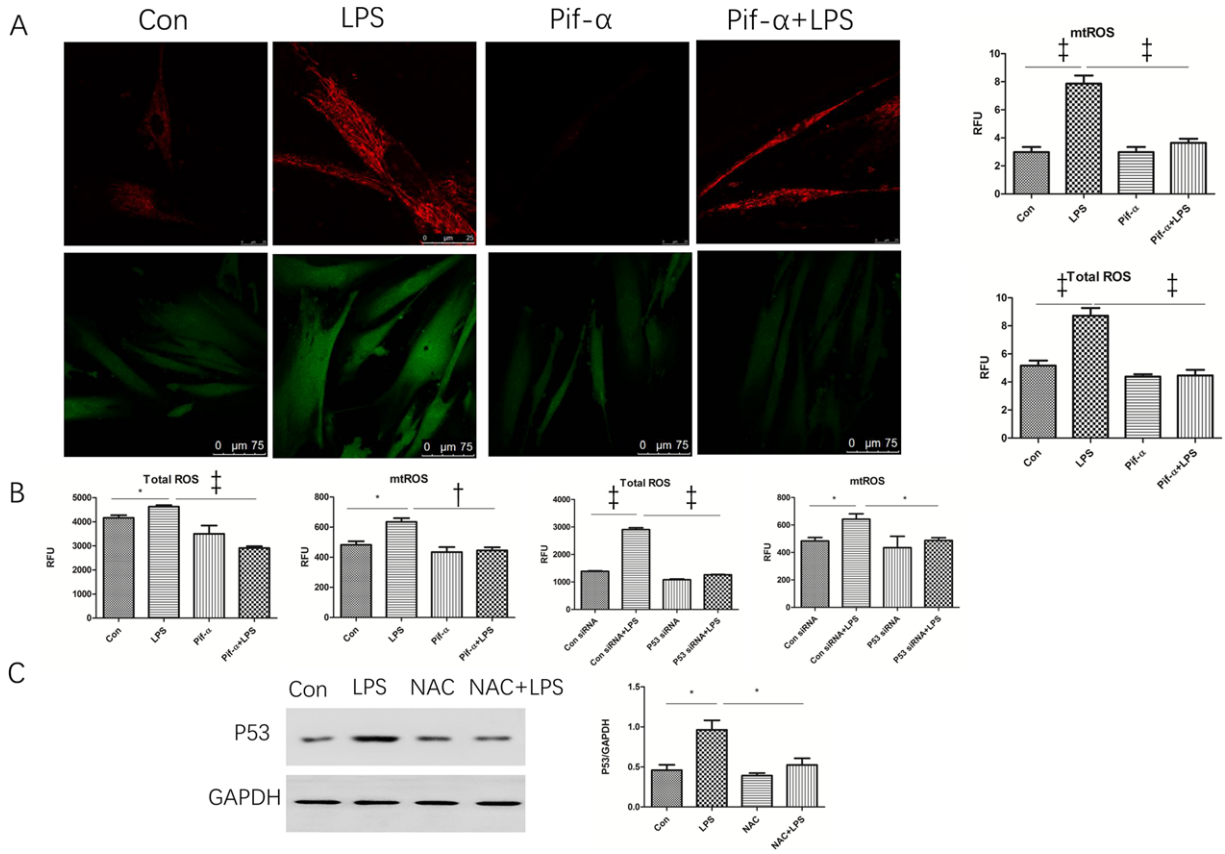

FIGURE 3 Activation of P53 regulated ROS levels in HGFs. ROS generation simultaneously enhanced P53 levels. HGFs were stimulated with LPS in the absence or presence of the inhibition of P53 inhibitor Pif-α or transfection with P53 and control siRNA and then incubated with cytoplastic ROS indicator H_2DCF-DA or mitochondrial ROS indicator MitoSOX Red, after which cytoplastic ROS and mitochondrial ROS levels were analyzed by (A) immunofluorescence microscopy, cytoplastic ROS (Scale bar 75 μm) mitochondrial ROS (Scale bar 25 μm) graph represented the average of MitoSOX-Red and H_2DCF-DA staining intensity of 25 cells (B) using a multimode microplate reader. Data were presented as the mean±SE ($n = 3$). (C) HGFs were stimulated with LPS in the absence or presence of NAC. The protein expression level of P53 was analyzed by Western blot with GAPDH as the internal marker. Results were further quantified by densitometric analysis. All experiments were performed 3 times. Values were presented as mean±SE ($n = 3$). Comparisons were analyzed by ANOVA, RFU: relative fluorescence unit, $^{*}P < 0.05$, $^{\dagger}P < 0.01$, $^{\ddagger}P < 0.001$

ROS both mediated proinflammatory cytokine generation in HGFs. We performed an enzyme-linked immunosorbent assay (ELISA) to detect TNF-α, IL-1β, and IL-6 levels. As shown in Figure 5, these cytokines were upregulated when HGFs were treated with LPS. Inhibition of P53 or ROS in the presence of LPS markedly decreased the proinflammatory cytokine levels in HGFs. Combined with the above experiments, our results indicated that the inflammatory state induced by LPS treatment was regulated through the P53-ROS pathway in HGFs.

3 | DISCUSSION

In this study, we report a novel role of P53 in LPS regulation of inflammation. P53 is the key tumor suppressor that promotes cell death and inhibits cell proliferation.[26,27] Its supportive role in inflammation by mediation of metabolic pathways is also recognized.[28,29] However, whether P53 regulates inflammatory responses in HGFs is still unclear. Our earlier report on mtROS in HGFs regulating the LPS-induced proinflammatory response[8] prompted us to continue investigating the relationship between P53 and ROS in HGFs. The present study demonstrated that LPS induced redox imbalance and proinflammatory cytokine release through P53 activation in HGFs; P53 mediated cellular respiration. And its interactions with mitochondria were followed by ROS generation and mitochondrial dysfunction. Therefore, our data strongly suggest that P53 acts as an important mediator of LPS-induced inflammation.

In HGFs, LPS commonly initiates its effect through pathogen-associated molecular patterns (PAMP). Most members of the toll-like receptor (TLR) family are recognized by LPS, leading to downstream inflammatory responses.[30] P53 reportedly plays a role in inflammation and immunity.[31,32] Recent evidence has demonstrated that P53 upregulates most TLRs and enhances TLR-dependent, proinflammatory cytokine production.[33,34] However, P53 stimulation of

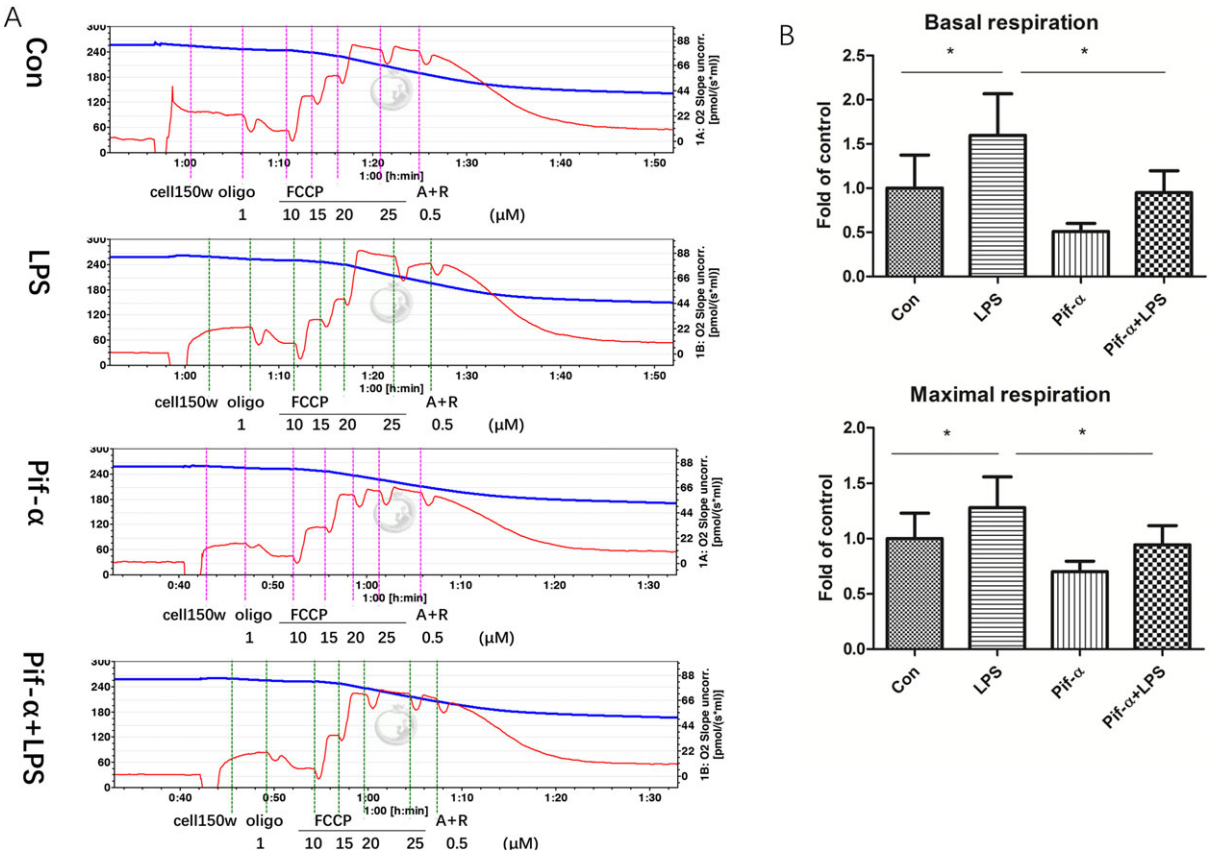

FIGURE 4 Activation of P53 regulated cell respiration. (A) LPS induced an increase of oxygen consumption rate in HGFs in contrast with control cells. Pif-α reversed LPS-induced increase in oxygen consumption rate in HGFs. (B) based on A paragraph, basal cell respiration and maximal respiration were calculated normalized to control groups. Oli: oligomycin, FCCP: carbonyl cyanide 4-(trifluoromethoxy) phenylhydrazone. R: rotenone, A: antimycin A. Values were mean±SE, $n = 4$. Data are representative of 4 independent experiments. Comparisons were analyzed by ANOVA. $^{*}P < 0.05$

TLRs is limited to human cells,[31] indicating that P53-related immune responses can only be detected in human cells. In addition, Lowe et al[35] illustrated that P53 and NF-κB coregulate proinflammatory gene responses in human macrophages. In the present study, we confirmed that P53 acts as an upstream signaling molecule for proinflammatory cytokine secretion and plays a pivotal role in the regulation of LPS-induced inflammation in HGFs.

Various studies have demonstrated that ROS play a significant role in the inflammatory response.[36,37] ROS overproduction after LPS treatment induces secretion of cytokines, including TNF-α, IL-1β, and IL-6, through the MAPK and NF-κB pathways in HGFs.[8] P53 also increased the levels of these three cytokines in our study. One possible mechanism for this phenomenon is that P53 regulates ROS production; our results suggested that P53 activation induced ROS production and ROS generation enhanced P53. Specifically, P53 inhibition by pifithrin-α pretreatment or P53 siRNA transfection suppressed LPS-induced ROS generation and cytokines expression in HGFs; and ROS suppression by NAC downregulated P53 expression and cytokine secretion, suggesting a regulatory role between P53 and ROS activation.

To address the role of P53 on ROS production, we investigated mechanisms accounting for ROS generation. A main source of ROS production is the respiratory chain in mitochondria, with increased OXPHOS resulting in increased ROS production.[14] Therefore, a new aspect of P53 as a regulator of energy metabolism has gained attention. P53 controls numerous metabolic enzymes that regulate ROS. One of its key functions is to augment cellular and mitochondrial respiration.[18] P53 promotes the conversion of pyruvate to acetyl-CoA, which enters the tricarboxylic acid cycle (TCA cycle) and enhances mitochondrial respiration via inhibiting the expression of PDK2, a negative regulator of PDH.[19] Our results suggest that PDK2 was potentially involved in P53-induced increased cellular respiration, because PDK2 significantly decreased in spite of a minor variation after LPS treatment and P53 activation. Moreover, in the presence of LPS stimulation, P53 inhibition slightly increased PDK2 expression and remarkably decreased cellular respiration and ROS generation, indicating the potential of P53 to modulate cellular redox homeostasis. These conditions may reveal that the LPS-induced, classical inflammatory response is partially dependent on P53, cellular respiration, and ROS production.

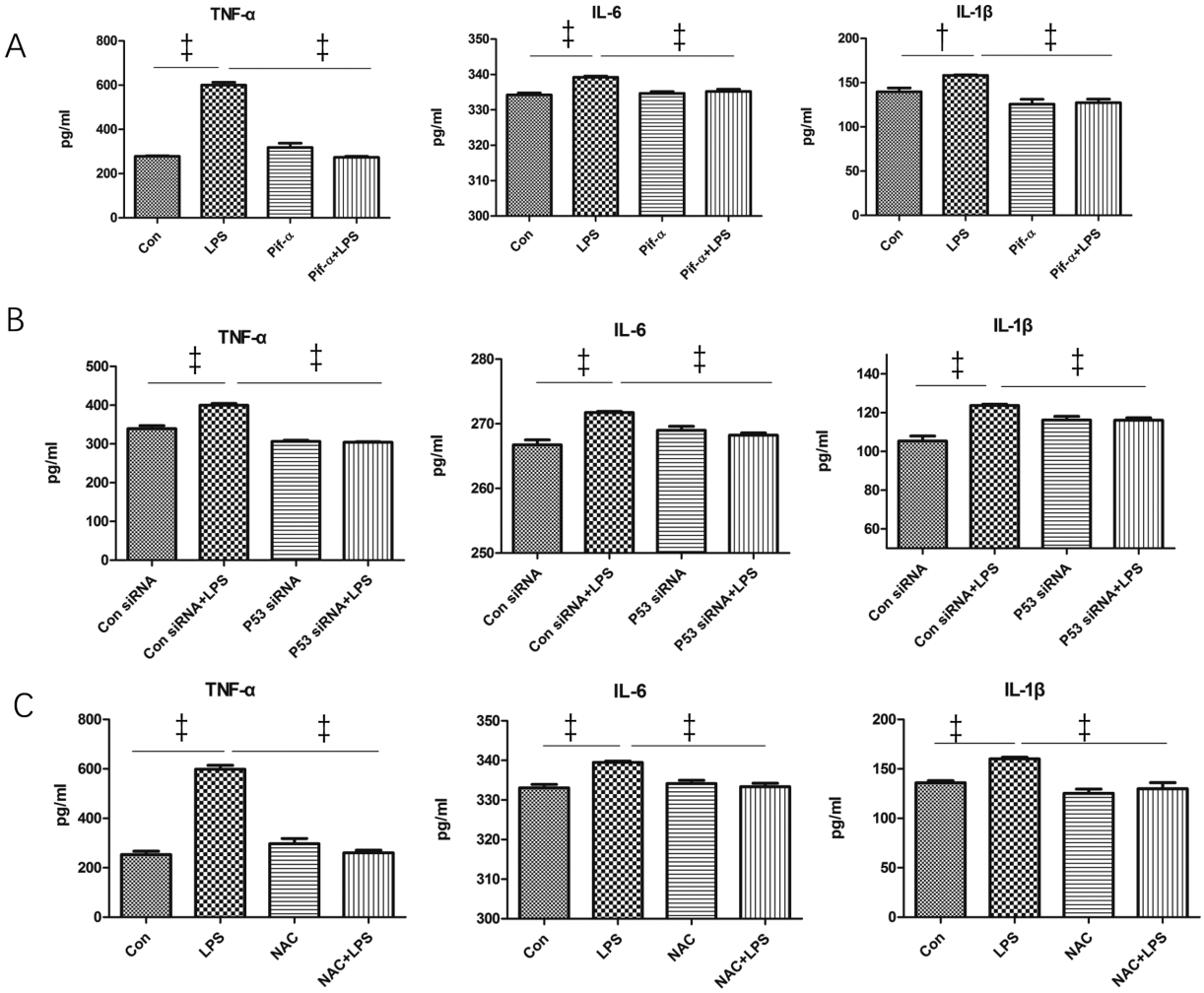

FIGURE 5 Proinflammatory cytokines secretion was significantly upregulated by LPS stimulation and downregulated by Pif-α or NAC addition together with LPS stimulation in HGFs. HGFs were treated with LPS in absence or presence of (A) inhibitor of P53 Pif-α or (B) transfection with P53 and control siRNA or (C) in the addition of NAC. The abundances of interleukin (IL)-1β, IL-6, and tumor necrosis factor (TNF)-α were measured by enzyme-linked immunosorbent assay (ELISA). Data were presented as the mean±SE ($n = 6$). Comparisons were analyzed by ANOVA. $^{\dagger}P < 0.01$, $^{\ddagger}P < 0.001$

Future research is required to describe whether PDK2 or other molecules are involved in this mechanisms of action.

In our initial experiments, we performed a P53-ROS signaling study to identify the role of P53 in LPS-induced inflammation. From an evolutionary perspective, ROS in mitochondria are an indicator of mitochondrial function. In addition to P53 expression, P53 localization in cells, and the relationship between P53 and mitochondria need to be elucidated. Under biologic conditions, P53 exhibits low activity and is subjected to a wide range of post-transcriptional modifications.[38,39] Certain stress signals drive the accumulation of P53 in the mitochondrial matrix,[25] where P53 interacts with cyclophilin D to initiate the mitochondrial permeability transition, which leads to mitochondrial membrane potential reduction and destruction.[40,41] The membrane permeability transition directly or indirectly enhances mitochondrial dysfunction, resulting in further redox imbalance and an inflammatory response in HGFs. LPS has been shown to trigger P53 activation and translocation to the mitochondria. Moreover, mitochondrial membrane potential destruction relies on P53 activity. Interestingly, our work revealed that mitochondrial dysfunction and cytokine release can be reversed by inhibition of P53 by pifithrin-α or siRNA when HGFs are stimulated by LPS.

4 | CONCLUSIONS

Based on these findings, it is conceivable that LPS-induced inflammation of HGFs, at least in part, occurs through the P53-ROS signaling pathway. Moreover, our first demonstration of interaction between P53 and ROS associated with HGF inflammation by LPS stimuli will provide additional therapeutic targets for rational periodontal treatment design.

ACKNOWLEDGMENTS

This work was supported in part by the National Natural Science Foundation of P. R. China (81271148) to Qingxian Luan, the National Natural Science Foundation of P. R. China (31371350) to Ming Zheng and the National Natural Science Foundation of P. R. China (81500863) to Xiaoxuan Wang. The authors declare no potential conflicts of interest with respect to authorship and/or publication of this article.

REFERENCES

1. Marcenes W, Kassebaum NJ, Bernabe E, et al. Global burden of oral conditions in 1990–2010: a systematic analysis. *J Dent Res*. 2013;92(7):592–597.
2. Dye BA, Global periodontal disease epidemiology. *Periodontol 2000*. 2012;58:10–25.
3. Pertersen PE, Ogawa H, The global burden of periodontal disease: towards integration with chronic disease prevention and control. *Periodontol 2000*. 2012;60:15-39.
4. Colombo AP, Boches SK, Cotton SL, et al. Comparisons of subgingival microbial profiles of refractory periodontitis, severe periodontitis, and periodontal health using the human oral microbe identification microarray. *J Periodontol*. 2009;80(9):1421–1432.
5. Dongari-Bagtzoglou AI, Ebersole JL, Increased presence of interleukin-6 (IL-6) and IL-8 secreting fibroblast subpopulations in adult periodontitis. *J Periodontol*. 1998;69(8):899–910.
6. Tabeta K, Yamazaki K, Akashi S, et al. Toll-like receptors confer responsiveness to lipopolysaccharide from *Porphyromonas gingivalis* in human gingival fibroblasts. *Infect Immun*. 2000;68(6):3731–3735.
7. Meng Z, Yan C, Deng Q, Gao D-F, Niu X-L, Curcumin inhibits LPS-induced inflammation in rat vascular smooth muscle cells in vitro via ROS-relative TLR4-MAPK/NF-κB pathways. *Acta Pharmacologica Sinica*. 2013;34(7):901–911.
8. Li X, Wang X, Zheng M, Luan QX, Mitochondrial reactive oxygen species mediate the lipopolysaccharide-induced pro-inflammatory response in human gingival fibroblasts. *Exp Cell Research*. 2016;347(1):212–221.
9. Naik E, Dixit VM, Mitochondrial reactive oxygen species drive proinflammatory cytokine production. *J Exp Med*. 2011;208(3):417–420.
10. Mukhopadhyay P, Horvath B, Zsengeller Z, et al. Mitochondrial reactive oxygen species generation triggers inflammatory response and tissue injury associated with hepatic ischemia-reperfusion: therapeutic potential of mitochondrially targeted anti-oxidants, *Free Radic Biol Med*. 2012;53(5):1123–1138.
11. Park J, Min JS, Kim B, et al. Mitochondrial ROS govern the LPS-induced pro-inflammatory response in microglia cells by regulating MAPK and NF-kappaB pathways, *Neurosci Lett*. 2015;584:191–196.
12. Sun X, Mao Y, Dai P, et al. Mitochondrial dysfunction is involved in the aggravation of periodontitis by diabetes. *J Clin Periodontol*. 2017;44:463–471.
13. Napa K, Baeder AC, Witt JE, et al. LPS from *P. gingivalis* negatively alters gingival cell mitochondrial bioenergetics. *Int J Dent*. 2017; 2697210.
14. Sabharwal SS, Schumacker PT, Mitochondrial ROS in cancer: initiators, amplifiers or an Achilles' heel? *Nat Rev Cancer*. 2014;14:709–721.
15. Park JY, Wang PY, Matsumoto T, et al. P53 improves aerobic exercise capacity and augments skeletal muscle mitochondrial DNA content. *Circ Res*. 2009;105(7):705–712.
16. Lebedeva MA, Eaton JS, Shadel GS, Loss of p53 causes mitochondrial DNA depletion and altered mitochondrial reactive oxygen species homeostasis. *Biochim Biophys Acta*. 2009;1787:328–334.
17. Saleem A, Carter HN, Hood DA, P53 is necessary for the adaptive changes in cellular milieu subsequent to an acute bout of endurance exercise. *Am J Physiol Cell Physiol*. 2014;306:241–249.
18. Kim HR, Roe JS, Lee JE, Cho EJ, Youn HD, P53 regulates glucose metabolism by miR-34a. *Biochem Biophys Res Commun*. 2013;437(2):225-231.
19. Contractor T, Harris CR, P53 negatively regulates transcription of the pyruvate dehydrogenase kinase pdk2. *Cancer Res*. 2012;72:560–567.
20. Zhang C, Lin M, Wu R, et al. Parkin, a p53 target gene, mediates the role of p53 in glucose metabolism and the Warburg effect. *Proc Natl Acad Sci USA*. 2011;108(39):16259–16264.
21. Yoshida Y, Shimizu I, Katsuumi G, et al. P53-induced inflammation exacerbates cardiac dysfunction during pressure overload. *J Mol Cell Cardiol*. 2015;85:183–198.
22. Shimizu I, Yoshida Y, Katsuno T, et al. P53-induced adipose tissue inflammation is critically involved in the development of insulin resistance in heart failure. *Cell Metab*. 2012;15(1):51–64.
23. Shimizu I, Yoshida Y, Moriya J, et al. Semaphorin 3E-induced inflammation contributes to insulin resistance in dietary obesity. *Cell Metab*. 2013;18(4):491–504.
24. Minamino T, Orimo M, Shimizu I, et al. A crucial role for adipose tissue p53 in the regulation of insulin resistance. *Nat Med*. 2009;15(9):1082–1087.
25. Vaseva AV, Moll UM, Identification of p53 in mitochondria. *Methods Mol Biol*. 2013;962:75–84.
26. Carvajal LA, Manfredi JJ, Another fork in the road–life or death decisions by the tumour suppressor p53. *EMBO Rep*. 2013;14(5):414–421.
27. Jackson JG, Post SM, Lozano G, Regulation of tissue- and stimulus-specific cell fate decisions by p53 in vivo. *J Pathol*. 2011;223(2):127–136.
28. Kawauchi K, Araki K, Tobiume K, Tanaka N, P53 regulates glucose metabolism through an IKK-NF-kappaB pathway and inhibits cell transformation. *Nat Cell Biol*. 2008;10(5):611–618.
29. Johnson RF, Perkins ND, Nuclear factor-κB, p53, and mitochondria: regulation of cellular metabolism and the Warburg effect. *Trends Biochem Sci*. 2012;37(8):317–324.
30. Kim YI, Park SW, Kang IJ, Shin MK, Lee MH, Activin suppresses LPS-induced toll-like receptor, cytokine and inducible nitric oxide synthase expression in normal human melanocytes by inhibiting NF-κB and MAPK pathway activation. *Int J Mol Med*. 2015;36(4):1165–1172.

31. Lane D, Levine A, P53 research: the past thirty years and the next thirty years. *Cold Spring Harb Perspect Biol*. 2010;2(12):a000893.
32. Munoz-Fontela C, Macip S, Martinez-Sobrido L, et al. Transcriptional role of p53 in interferon-mediated antiviral immunity. *J Exp Med*. 2008;205(8):1929–1938.
33. Menendez D, Shatz M, Azzam K, Garantziotis S, Fessler MB, Resnick MA, The toll-like receptor gene family is integrated into human DNA damage and p53 networks. *PLoS Genet*. 2011;7(3):e1001360.
34. Shatz M, Menendez D, Resnick MA, The human TLR innate immune gene family is differentially influenced by DNA stress and p53 status in cancer cells. *Cancer Res*. 2012;72(16):3948–3957.
35. Lowe JM, Menendez D, Bushel PR, et al. P53 and NF-κB coregulate proinflammatory gene responses in human macrophages. *Cancer Res*. 2014;74(8):2182–2192.
36. West AP, Brodsky IE, Rahner C, et al. TLR signaling augments macrophage bactericidal activity through mitochondrial ROS. *Nature*. 2011;472(7344):476–480.
37. Agod Z, Fekete T, Budal MM, et al. Regulation of type I interferon responses by mitochondria-derived reactive oxygen species in plasmacytoid dendritic cells. *Redox Biol*. 2017;13:633–645.
38. Gu B, Zhu WG, Surf the post-translational modification network of p53 regulation. *Int J Biol Sci*. 2012;8(5):672–684.
39. Kruse JP, Gu W, Modes of p53 regulation. *Cell*. 2009;137(4):609–622.
40. Vaseva AV, Marchenko ND, Ji K, Tsirka SE, Holzmann S, Moll UM, P53 opens the mitochondrial permeability transition pore to trigger necrosis. *Cell*. 2012;149(7):1536–1548.
41. Yuan J, Ding PW, Yu M, et al. IL-17 induces MPTP opening through ERK2 and p53 signaling pathway in human platelets. *J Huazhong Univ Sci Technolog Med Sci*. 2015;35(5):679–683.

How to cite this article: Liu J, Zeng J, Wang X, Zheng M, Luan Q. P53 mediates lipopolysaccharide-induced inflammation in human gingival fibroblasts. *J Periodontol*. 2018;89:1142–1151. https://doi.org/10.1002/JPER.18-0026